PRL-1 Tyrosine Phosphatase Regulates c-Src Levels, Adherence, and Invasion in Human Lung Cancer Cells

Hiroyuki Achiwa and John S. Lazo

Department of Pharmacology, Drug Discovery Institute, and University of Pittsburgh Cancer Institute, University of Pittsburgh, Pittsburgh, Pennsylvania

Abstract

Phosphatases of regenerating liver (PRL) constitute a subfamily of the protein tyrosine phosphatases that are implicated in oncogenic and metastatic phenotypes. In this study, we evaluated the role of PRL-1 in cell proliferation and metastatic processes in human lung cancer cells. We stably transfected human A549 lung cancer cells with several short hairpin RNAs for PRL-1 and found decreased invasive activity in the resulting clones compared with control cells. In addition, cells with suppressed PRL-1 exhibited greater adherence and cell spreading on fibronectin and a decreased proliferation rate compared with control cells. To address possible mechanisms for the altered phenotypes, we examined known biochemical regulators of adhesion and invasion. Inhibition of PRL-1 decreased c-Src and p130Cas expression and Rac1 and Cdc42 activation without any apparent modification of focal adhesion kinase (FAK) expression. Total tyrosine FAK phosphorylation and Tyr^{397} phosphorylation levels were continuously elevated in PRL-1 knockdown cells plated on fibronectin. In immunofluorescence studies, reduction in PRL-1 seemed to decrease cell membrane protrusions with a reduction in actin fiber extensions in spite of continuous phosphorylation of Tyr^{397} FAK, which could reflect reduced adhesion turnover. Our data implicate PRL-1 in the fundamental process of cell adhesion and migration in human lung cancer cells by affecting Rac1, Cdc42, and c-Src activation. These results support the hypothesis that PRL-1 plays an important role in maintaining the malignant phenotype by exploiting Src activation processes, and that PRL-1 could be a promising therapeutic target for cancer metastasis and cell growth. [Cancer Res 2007;67(2):643–50]

Introduction

Lung cancer is currently the leading cause of cancer-related death in both men and women in the United States, accounting for >160,000 deaths per year (1). Despite numerous clinical attempts to control lung cancer, the 5-year survival remains <15% (1). The fundamental cause of patient morbidity is the development of metastasis. Regrettably, the biochemical basis for metastatic development remains poorly understood mainly because metastasis is a highly complex process and involves a variety of positive and negative factors (2). Protein tyrosine phosphorylation is critical for regulating the signaling pathways involved in tumor cell adhesion, invasion, and metastasis. Protein tyrosine phosphatases (PTP), such as PTPα, PTP1B, or PTP-PEST, have been implicated in processes that are essential for tumor cell metastasis due to their ability to affect focal adhesion regulation and cell migration (3–5). The phosphatase of regenerating liver (PRL) family of PTPs also seems to have an important role in the basic biology of cancer cell development and metastasis (6). PRL-1 (also known as PTP4A1 and PTP*CAAX*) was first identified as an immediately-early gene whose expression was induced in rat regenerating liver (7); this was followed by the identification of PRL-2 and PRL-3, with which PRL-1 shares 87% and 75% sequence identity, respectively (8). Saha et al. (9) compared gene expression profiles in colon cancers that had metastasized to the liver with those in primary tumors and normal colon cells and found that PRL-3 was overexpressed (9, 10). In addition, high PRL-3 mRNA expression was reported in metastatic lesions derived from colorectal cancers regardless of the site of metastasis, whereas low PRL-3 mRNA levels were observed in non-colorectal cancer metastases to the lung or the liver (10). PRL-1 is expressed in normal lung bronchiolar epithelium (11) and is overexpressed in many histologically distinct, cultured, human, tumor cell lines, including lung cancer cells (12). Several studies show that cells expressing high levels of PRL-1 exhibit an enhanced proliferation rate (11, 13, 14). Chinese hamster ovary cells stably expressing PRL-1 or PRL-3 have enhanced cell motility and invasiveness; cells with elevated PRL-1 or PRL-3 have an increased capacity to produce metastatic tumors in mice (15). Furthermore, pancreatic ductal epithelial cells stably overexpressing PRL-1 and PRL-2 exhibited a transformed phenotype in culture and tumor growth in nude mice (16).

Initially, the substrates for PRL-1 were thought to be nuclear because PRL-1 was originally described as a nuclear protein when ectopically expressed in transfected cells (17). Subsequently, Zeng et al. (13) reported that PRL phosphatases were localized to the plasma membrane and early endosomes, and that the localization pattern was dependent on their posttranslational farnesylation. Recently, Fiordalisi et al. (18) reported that PRL-1 and PRL-3 promoted motility and invasion in colon cancer cells by stimulating Rho signaling pathways using transfection approaches. Kato et al. (19) also found that transient reduction of PRL-1 or PRL-3 abrogated colon cancer cell motility and hepatic colonization. To elucidate the functional role of PRL-1 phosphatase in tumor metastasis, we have studied lung cancer cells in which PRL-1 has been depleted using short hairpin RNA (shRNA) technology.

Herein, we report that endogenous PRL-1 silencing inhibited lung cancer cell invasion with decreased expression of c-Src and p130Cas and inactivation of Rac1 and Cdc42. These results reveal a novel role of PRL PTPs in regulating fundamental signals important for cancer cell metastasis and encourage greater attention on this class of PTP.

Requests for reprints: John S. Lazo, Department of Pharmacology, University of Pittsburgh, Biomedical Science Tower 3, Suite 10040, 3501 Fifth Avenue, Pittsburgh, PA 15260. Phone: 412-648-9200; Fax: 412-648-9009; E-mail: lazo@pitt.edu.

doi:10.1158/0008-5472.CAN-06-2436

Materials and Methods

Cell line, antibodies, and reagents. A549 cells were purchased from the American Type Culture Collection (Manassas, VA). Antibodies and reagents were obtained from the following sources: goat anti-PRL-1 polyclonal antibody (Everest Laboratory, Oxfordshire, United Kingdom); anti–focal adhesion kinase (anti-FAK; clone 77), anti-p130Cas (clone 21), anti-paxillin (clone 165), and anti-Csk (clone 52) monoclonal antibodies and glutathione agarose beads (BD Transduction Laboratories, San Diego, CA); anti-c-Src (SRC2), anti-c-Src (H12), and anti-c-Myc (9E10) antibodies and Protein A/G PLUS-Agarose immunoprecipitation reagent (Santa Cruz Biotechnology, Santa Cruz, CA); phospho-specific antibodies to Tyr^{397} FAK and Tyr^{418} Src and Tyr^{529} Src (Biosource International, Camarillo, CA); phospho-specific antibody to Tyr^{925} FAK (Cell Signaling Technology, Beverly, MA); and anti-Rac1 and anti–phosphorylated tyrosine (pTyr; 4G10) monoclonal antibodies and the Rac/Cdc42 activation kit (Upstate Biotechnology, Lake Placid, NY).

shRNA. To deplete endogenous PRL-1, we selected three different 21-nucleotide sequences according to the manufacturer's instructions and software:[1] AAGCAACTTATGACACTACTC (PRL-1 silencing site 149), AACCAGATTGTTGATGACTGG (PRL-1 silencing site 232), AACAGCAAGCAACTTCTGTAT (PRL-1 silencing site 424). The numbers 149, 232, and 424 indicate the starting nucleotide number of shRNA-targeting sequences on the coding PRL-1 mRNA based on the published sequence data from Genbank (accession no. NM_003463). The specificity of each sequence was verified by a BLAST search of the public databases. p*Silencer* 4.1-CMV puro expression vectors (Ambion, Austin, TX) that produce shRNAs targeted against PRL-1 (named PRL-1-149i, PRL-1-232i, and PRL-1-424i) were also prepared according to the manufacturer's instructions. In brief, three sets of oligonucleotides were chemically synthesized: PRL-1-149 sense, 5′-GATCCGCAACTTATGACACTACTCTTCAAGAGAGAGTAGTGTCATAAGTTGCTTA-3′; PRL-1-149 antisense, 5′-AGCTTAAGCAACTTATGACACTACTCTCTCTTGAAGAGTAGTGTCATAAGTTGCG-3′; PRL-1-232 sense, 5′-GATCCCCAGATTGTTGATGACTGGTTCAAGAGACCAGTCATCAACAATCTGGTTA-3′; PRL-1-232 antisense, 5′-AGCTTAACCAGATTGTTGATGACTGGTCTCTTGAACCAGTCATCAACAATCTGGG-3′; PRL-1-424 sense, 5′-GATCCCAGCAAGCAACTTCTGTATTTCAAGAGAATACAGAAGTTGCTTGCTGTTA-3′; and PRL-1-424 antisense, 5′-AGCTTAACAGCAAGCAACTTCTGTATTCTCTTGAAATACAGAAGTTGCTTGCTGG-3′ (the underlined sequences contribute to forming shRNAs). The annealed oligonucleotides encoding shRNAs were then subcloned into the *Bam*HI-*Hin*dIII site of the p*Silencer* 4.1-CMV puro vector. For transfection, 1×10^5 cells were plated in six-well plates 24 before transfection in normal growth medium. Four micrograms of plasmid DNA and 250 μL LipofectAMINE 2000 (Invitrogen, Carlsbad, CA) were combined with 500 μL Opti-MEM I reduced-serum media (Invitrogen), incubated for 20 min at room temperature, and added to each well. After 24 h, the medium was replaced with basal medium Eagle (Invitrogen) with 2 μg/mL puromycin and 10% fetal bovine serum (FBS). After 2 weeks, stable round colonies were harvested and cloned by limiting dilution method.

RNA isolation and reverse transcription-PCR. Total RNA was extracted with the RNeasy Mini kit (Qiagen, Valencia, CA) according to the manufacturer's instructions. Reverse transcription-PCR (RT-PCR) for PRL-1, PRL-2, PRL-3, and glyceraldehyde-3-phosphate dehydrogenase (GAPDH) as an internal control was carried out in a volume of 50 μL by SuperScript III One-step RT-PCR System (Invitrogen) as per manufacturer's instruction. Following primer pairs were used for each reaction: PRL-1, 5′-ACCTGGTTGTTGTATTGCTGTT-3′ (forward) and 5′-GTTGTTTCTATGACCGTTGGAA-3′ (reverse); PRL-2, 5′-AGCCAGGTTGCTGTGTTGCAG-3′ (forward) and 5′-CACAGCAATGCCCATTGGTA-3′ (reverse); PRL-3, 5′-AAGGTAGTGGAAGACTGGCT-3′ (forward) and 5′-GGTGAGCTGCTTGCTGTTGAT-3′ (reverse); GAPDH, 5′-GATGGGTGTGAACCATGAGA-3′ (forward) and 5′-CAGGGATGATGTTCTGGAGA-3′ (reverse).

[1] http://www.ambion.com/techlib/misc/siRNAfinder.html.

Lysis buffers, immunoprecipitations, Western blotting, and GTPase activation assay. Cells were lysed in modified radioimmunoprecipitation assay (RIPA) buffer containing 0.1% SDS, 1% Triton X-100, protease inhibitors (10 μg/mL leupeptin, 10 μg/mL apoprotein, 100 μg/mL AEBSF, 10 μg/mL soybean trypsin inhibitor, 1 mmol/L phenylmethylsulfonyl fluoride), and phosphatase inhibitors (2 mmol/L Na_3VO_4, 12 mmol/L β-glycerol phosphate, and 10 mmol/L NaF). For immunoprecipitation, cells were lysed in modified RIPA buffer containing 0.05% SDS, 1% Triton X-100, protease inhibitors, and phosphatase inhibitors. Antibodies for immunoprecipitation (1–2 μg) were incubated with lysates (500 μg of protein) for 1 h at 4°C and were collected with 20 μL of Protein A/G PLUS-Agarose (Santa Cruz Biotechnology) for 1 h at 4°C. The immunoprecipitates were washed thrice with PBS followed by standard Western blotting procedures. The Rac and Cdc42 activation assays were done according to the manufacturer's instructions (Upstate Biotechnology). Briefly, cells were plated and lysed after 2 days of growth on fibronectin or noncoated dishes using a Mg lysis buffer supplemented with phosphatase inhibitors and protease inhibitors as described above. The cell lysate for the Rac activation assay was precleared for 10 min with glutathione *S*-transferase (GST) agarose beads (BD PharMingen, San Diego, CA). Lysates were then incubated with PAK-1 PBD-agarose for 45 min at 4°C. Beads were washed thrice with Mg lysis buffer, and samples were prepared for Western blotting. GTP-bound Rac1 and Cdc42 were identified by blotting with anti-Rac1 and anti-Cdc42 antibodies, respectively.

Cell proliferation, migration, and invasion assays. Cell proliferation was determined by trypan blue staining and cell counting. Cell motility assay was done using Transwell (6.5-mm diameter, 8-μm pore size polycarbonate membrane) obtained from Corning (Cambridge, MA). Cells (1×10^5) in 0.5 mL serum-free medium were placed in the upper chamber, and the lower chamber was loaded with 0.8 mL medium containing 10% FBS. Cells that migrated to the lower surface of filters were stained with Wright Giemsa solution, and five fields of each well were counted after 4 to 24 h of incubation at 37°C with 5% CO_2. Three wells were examined for each condition and cell type, and the experiments were repeated thrice. The cell invasion assay was conducted using BD Biocoat Matrigel 24-well invasion chambers with filters coated with extracellular matrix on the upper surface (BD Biosciences, Bedford, MA). Control inserts were used for migration control. The experiments were done according to the manufacturer's protocol. We added 2.5×10^4 cells in 0.5 mL of serum-free culture medium to the upper chamber, and after incubation at 37°C for 24 h, we stained cells and determined total cell invasion and migration as described above. Invasiveness was expressed as the percent invasion for each cell type through the Matrigel matrix and membrane relative to the migration through the control membrane.

Cell adhesion and spreading assays. For cell adhesion, 2×10^5 cells were plated on noncoated, collagen I–, fibronectin-, or laminin-precoated 12-well culture plates (BD Biosciences) at 37°C with 5% CO_2. After a 60-min incubation, nonadherent cells were removed by washing twice with PBS. Adherent cells were stained with Wright Giemsa solution. For cell spreading assay, 1×10^6 cells were plated on extracellular matrix–precoated 35-mm culture dishes (BD Biosciences). Cells were allowed to spread for 30 to 120 min. Spread cells were defined as cells with extended process, lacking a round morphology and phase dim, whereas nonspread cells were rounded and phase bright under a phase-contrast microscope. For both adhesion and spreading assays, five fields in three wells or dishes were counted, and each experiment was repeated thrice.

Immunofluorescence. Cells were seeded on fibronectin-coated culture plate and fixed at the indicated time points with 4% paraformaldehyde at room temperature for 10 min. After three washes with PBS, cells were permeabilized for 5 min with 0.1% Triton X-100. After blocking with 1% bovine serum albumin, cells were incubated with the anti-$pTyr^{397}$ FAK antibody for 2 h followed by incubation with Alexa Fluor 488–conjugated anti-rabbit IgG for $pTyr^{397}$ FAK and rhodamine phalloidin for actin organization (Invitrogen). The fluorescence images of cells were captured and analyzed using an ArrayScan VTI (Cellomics, Inc., Pittsburgh, PA).

Results

PRL-1 silencing by shRNA. To address the function of endogenous PRL-1 in lung cancer cells known to express high levels of PRL-1 (12), we established A549 cells that stably expressed shRNA for PRL-1. Three different 21-nucleotide sequences were selected for shRNA and were named according to the starting nucleotide number of the targeting sequence: 149i, 232i, and 424i. We isolated four A549-149i, three A549-232i, three A549-424i, and three scramble RNA–transfected (A549-SCR) clones. Three of A549-149i and one of A549-232i showed decreased PRL-1 mRNA levels, and no A549-424i clones showed PRL-1 silencing (data not shown). One clone made with each of the two targeting sequences that persistently exhibited suppressed PRL-1 expression were selected and renamed 149i and 232i; one of the SCR clones was also used as a control for this study. In 149i and 232i cells chronically expressing PRL-1 shRNA, PRL-1 protein levels were decreased 66% and 40%, respectively, whereas they were not decreased in SCR shRNA-expressing cells (Fig. 1*A, top*). To confirm the antibody specificity to PRL-1, we loaded GST fusion PRL family proteins on SDS-PAGE and blotted with an anti-PRL-1 antibody. As shown in Fig. 1*A* (*bottom*), the antibody showed no cross-reactivity to human PRL-2 or PRL-3. The PRL-1 knockdown 149i and 232i cells did not show any obvious effect on PRL-2 and PRL-3 mRNA expression levels but displayed a 30% to 40% decrease in PRL-1 mRNA (Fig. 1*B*).

Compared with parental cells or scrambled transfectants (Fig. 1*C, a, b*, and *e*), PRL-1 knockdown clones (Fig. 1*C, c, d*, and *f*) displayed extended or elongated cytoplasm with spindle-shaped nuclei. These differences while sometimes subtle were seen both with short-term incubation (Fig. 1*C, e* and *f*) and in nearly confluent cells (*a–d*). We next examined the effect of PRL-1 knockdown on cell proliferation. The 149i cells proliferated more slowly than parental or control cells, and the 232i cells, which had intermediate PRL-1 silencing (Fig. 1*A*), also did not grow as rapidly as parental or control cells (Fig. 1*D*).

PRL-1 silencing decreased cell invasiveness. To investigate the role of PRL-1 in cancer cell metastatic processes, we did cell migration and invasion assays using Transwell migration and Matrigel invasion chambers, respectively. Surprisingly, PRL-1–silenced clones migrated faster at 4 and 8 h than did control cells in the cell migration assay (Fig. 2*A* and *B*). By 24 h, however, control cells achieved the same number of migrated cells per field as did the PRL-1 shRNA clones, suggesting that the initial elevated migration in PRL-1 knockdown cells might reflect altered adhesion. With the invasion assay, PRL-1–silenced clones invaded significantly less than the parental cells or scramble cells (Fig. 2*C* and *D*).

PRL-1 knockdown enhanced cell adhesion and spreading on fibronectin. The morphologic changes and migration results suggested that loss of PRL-1 expression might alter cell adherence, spreading, or cytoskeleton structure. To assess the adhesion on various extracellular matrix, we did adhesion assay using non-coated or precoated culture dishes with various extracellular

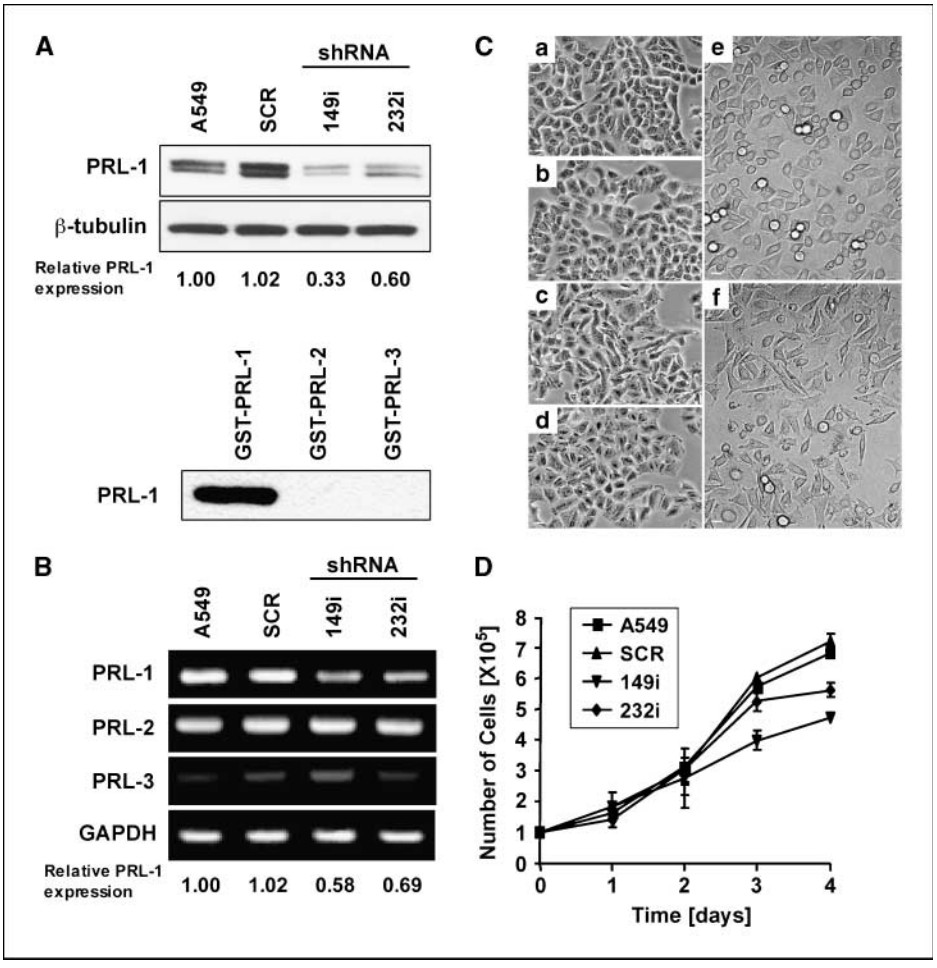

Fig. 1. A549-149i and A549-232i cells had reduced PRL-1 levels, altered morphology, and reduced proliferation rates. The cell clone numbers 149 and 232 indicate the starting nucleotide number of shRNA-targeting sequences of PRL-1 mRNA. PRL-1 shRNA decreased both protein (*A, top*) and mRNA (*B*) levels. β-Tubulin and GAPDH were used as internal controls for protein and mRNA, respectively. Western blotting and RT-PCR images were processed and quantified by the public domain program ImageJ 1.36b, written by Wayne Rasband (National Institute of Mental Health, Bethesda, MD). Protein expression relative to β-tubulin and mRNA levels relative to GAPDH. Average fold changes from three independent experiments normalized to parental A549 cells. *A, bottom,* anti-PRL-1 antibody specificity to PRL-1 was confirmed by Western blot with recombinant GST-PRL protein. *B,* shRNA for PRL-1 did not influence PRL-2 or PRL-3 mRNA levels. *C,* compared with parental A549 cells (*a*) or scrambled transfectants (*b* and *e*), the PRL-1–inhibited 149i (*c* and *f*) and 232i (*d*) cells displayed slightly more elongated cell shape with spindle-like nuclei. Nearly confluent cell cultured on plastic dishes (*a–d*) or phase-contrast images of adherent cells 3 h after seeding on fibronectin-coated glass strips (*e* and *f*). Bar, 20 μm. *D,* PRL-1 knockdown cells had reduced proliferation rates compared with control cells. *Points,* average cell numbers of triplicate determination repeated three independent times; *bars,* SE.

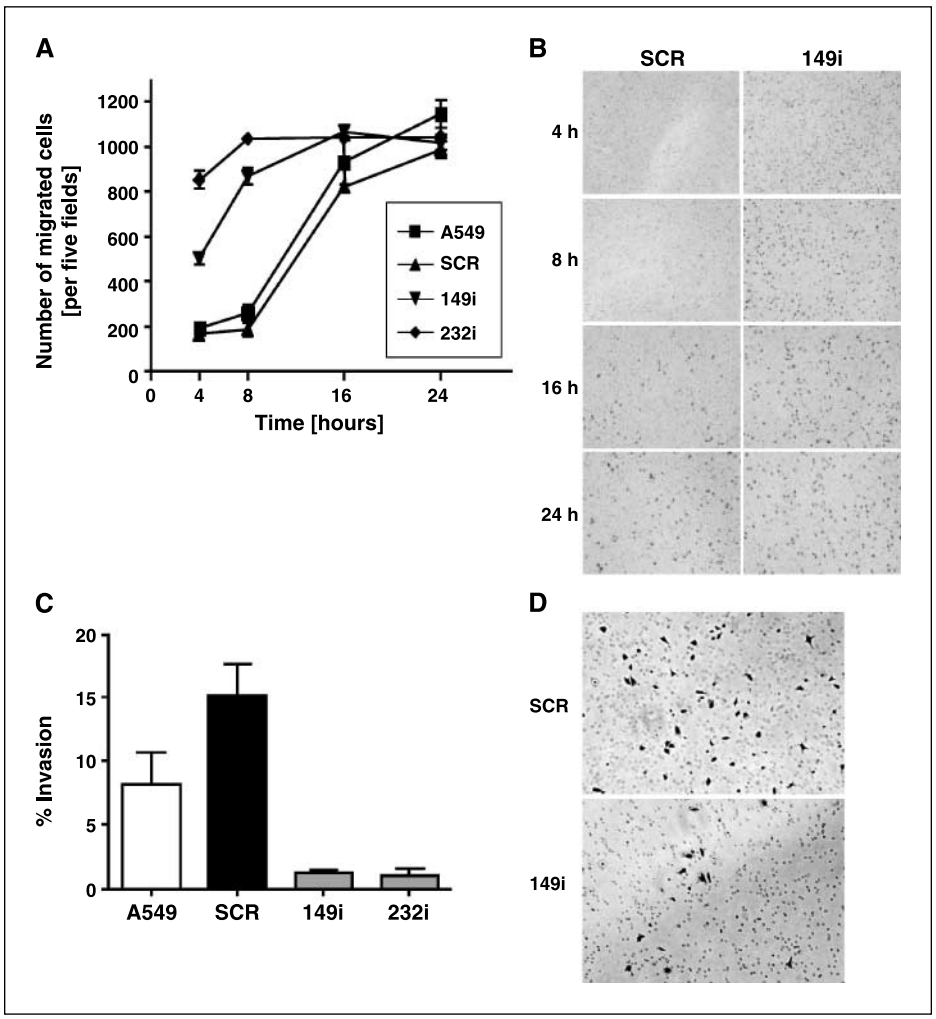

Fig. 2. Loss of PRL-1 inhibited cell migration and invasion. *A,* time course of migration of A549 cells with normal or inhibited PRL-1. After various indicated times, cells that migrate to the lower chamber were fixed, stained, and counted using a light microscope. *Points,* mean of independent experiments measured in triplicate and repeated three times for each cell type; *bars,* SE. *B,* representative images of SCR and 149i cells on the lower side of a membrane at different time points in the migration assay. *C,* invasion after loss of PRL-1. Invasive activity was determined as the percent invasion through Matrigel matrix and membrane relative to the migration through the control membrane. *Columns,* mean of independent experiments measured in triplicate and repeated three independent times; *bars,* SE. *D,* representative images of SCR and 149i cells on the lower side of a membrane 24 h after plating for the invasion assay.

matrix, including collagen I, fibronectin, and laminin. Sixty minutes after cell plating, we quantified the number of adherent cells with each extracellular matrix–coated plate. As shown in Fig. 3*A*, PRL-1 knockdown cells showed more adherence than control cells on fibronectin, although all populations clearly have a preference for noncoated or collagen-coated dishes. On laminin-coated dishes, PRL-1 knockdown cells showed slightly fewer adherent cells than control cells, whereas on noncoated and collagen I–coated dishes, there were no clear differences among the cell populations (Fig. 3*A*).

Next, we did a cell spreading assay on collagen I–, fibronectin-, and laminin-precoated and noncoated cell culture dishes for 30, 60, and 120 min. On fibronectin, PRL-1–deficient cells showed significantly faster cell spreading than control cells (Fig. 3*B, left* and *C*). On noncoated dishes (Fig. 3*B, right*) and collagen I– or laminin-precoated dishes (data not shown), fewer cells attached, and there were no significant differences with cell spreading among these cell types.

PRL-1 knockdown decreased c-Src and p130Cas expression independent of FAK. To investigate the molecular mechanisms of PRL-1 cell adhesion, spreading, migration, and invasion, we examined the effect of PRL-1 knockdown on focal adhesion and downstream pathways. As shown in Fig. 4*A*, PRL-1 knockdown did not influence FAK expression, FAK phosphorylation status, and $pTyr^{397}$ FAK or FAK interaction with c-Src as measured by coimmunoprecipitation. Interestingly, c-Src expression was markedly decreased in PRL-1 knockdown clones both with and without fibronectin stimulation. To examine c-Src stimulative ($pTyr^{418}$) or regulatory ($pTyr^{529}$) phosphotyrosine status, we immunoprecipitated c-Src. Overall, c-Src tyrosine phosphorylation seemed not to change. We found in cells grown on noncoated plates that both $pTyr^{418}$ and $pTyr^{529}$ Src levels decreased approximately proportional to the decrease in c-Src protein levels in PRL-1–depleted cells (Fig. 4*A*). We conclude suppression of PRL-1 protein levels decreased c-Src expression with no apparent modification in the phosphorylation status of c-Src. Reduction of PRL-1 protein levels also decreased p130Cas levels in cells both with and without fibronectin stimulation. Paxillin expression was undetectable in cells grown in the absence of extracellular matrix, irrespective of the PRL-1 levels, whereas cells stimulated with fibronectin had prominent paxillin expression that was suppressed in PRL-1 knockdown cells.

PRL-1 knockdown altered actin organization, lamellipodia extension, and Rac1 and Cdc42 activation. We hypothesized that PRL-1 expression was associated with c-Src activity and with the downstream Rho family GTPases, such as Rac1 or Cdc42, which are involved in regulating cell migration. In addition, we hypothesized that PRL-1 knockdown could delay adhesion

turnover via c-Src inhibition. Thus, we examined the kinetics of interaction among putative participants in focal adhesion turnover in response to cell attachment to fibronectin in SCR and 149i cells. The levels of $pTyr^{418}$ Src increased within 2 h in the SCR cells but did not increase in 149i cells (Fig. 4*B*). We observed phosphotyrosine FAK, $pTyr^{397}$ and $pTyr^{925}$ FAK, and expression of paxillin, c-Src, Csk, and p130Cas increased in a time-dependent manner in control cells placed on fibronectin. In contrast, in 149i cells, high levels of phosphotyrosine FAK and $pTyr^{397}$ FAK and moderate levels of $pTyr^{925}$ FAK were seen at 30 min after fibronectin stimulation and persisted for 120 min. In addition, undetectable or low levels of paxillin, c-Src, and p130Cas were seen in 149i cells throughout the kinetic study (Fig. 4*B*). Tyrosine-phosphorylated paxillin was induced time-dependently in both cells, although the basal level phosphorylated paxillin was higher in 149i (Fig. 4*B*). Persistent phosphorylation of FAK and paxillin would be consistent with decreased adhesion turnover in PRL-1 knockdown cells.

We next examined microscopically the distribution of phosphorylated FAK and actin organization following PRL-1 silencing (Fig. 5*A*). In PRL-1 knockdown 149i cells attached to fibronectin for 60 min, $pTyr^{397}$ FAK distributed throughout the entire cell with high intensity spots in the cell periphery (Fig. 5*A, f*), and after 240 min, it distributed along with the actin stress fibers (Fig. 5*A, l*). This contrasted with SCR cells, which showed a peripheral distribution at 60 min but subsequently distributed predominantly to the central area and lamellipodium at 240 min (Fig. 5*A, g* and *i*). Remarkably, $pTyr^{397}$ FAK staining predominated over actin staining in the cell spreading leading edge in 149i cells especially when compared with SCR cells (Fig. 5*A, c* and *i*), which would be consistent with focal adhesion occurring before actin extension and lamellipodium protrusion with the spreading of PRL-1 knockdown cells.

Finally, to examine the possible role of PRL-1 in modifying Rho family GTPase activity, which participates in cell migration involving focal adhesion rearrangement and actin cytoskeletal reorganization, we measured Rac and Cdc42 activation. As shown in Fig. 5*B*, Rac-GTP was decreased in PRL-1 knockdown cells stimulated by fibronectin. GTP-Cdc42 also was markedly decreased on fibronectin in 149i and 232i cells (Fig. 5*B*). PRL-1 knockdown had no effect on the total expression of Rac1 or Cdc42.

Discussion

Clinical correlative, ectopic overexpression and transient suppression studies all support a functional role for PRL-1 in cancer cell invasion and metastasis. As a complementary alternative, we have developed lung cancer cells in which PRL-1 was selectively and stably depleted by shRNA and observed suppressed cell invasion with enhanced cell adherence and spreading. We hypothesize that these phenotypic changes resulted from delayed adhesion turnover involving decreased c-Src expression and inactivation of Rac1 and Cdc42. PRL-1 stably silenced clones, which morphologically had elongated cytoplasm compared with control cells, were less invasive than control cells (Fig. 2*C* and *D*). Cell adhesion is mediated mainly through the engagement of integrins with the extracellular matrix, including fibronectin, collagen, and laminin. The PRL-1 knockdown cells were more adherent and had enhanced spreading especially on fibronectin, which is common in pulmonary tissue (Fig. 3*A–C*). These results support a role for PRL-1 in cell-extracellular matrix interactions particularly with regard to the pathways from integrins and focal adhesion complex to the downstream cell adhesion and migration processes. Recent studies by Peng et al. (20) suggest the PRL-1–related phosphatase PRL-3 interacts with integrin α_1 and regulates integrin β_1 and extracellular signal-regulated kinase 1/2 (Erk1/2) phosphorylation. The preference of PRL-1–depleted cells to bind to fibronectin suggests PRL-1 regulates a different extracellular matrix interaction than PRL-3 because integrins α_1 and β_1 are receptors for collagen and laminin but not fibronectin. Kato et al. (19)

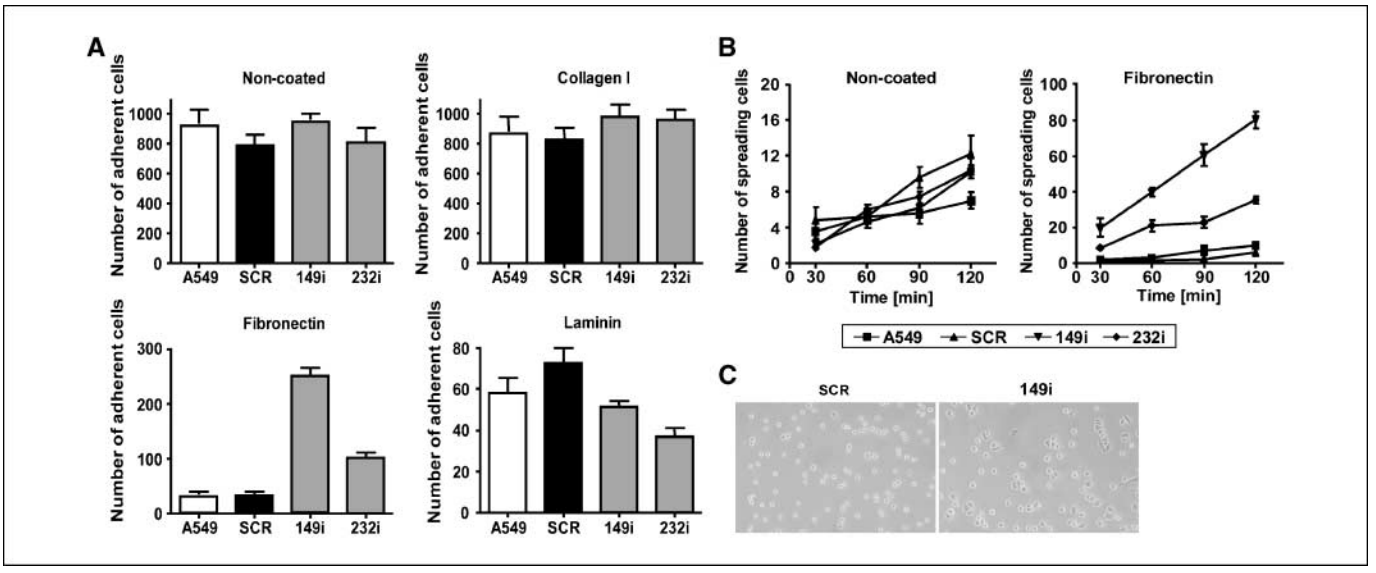

Fig. 3. PRL-1 silencing enhanced cell adhesion and spreading on fibronectin. *A,* cell adhesion on fibronectin was enhanced in PRL-1–inhibited cells compared with parental and control cells. After a 60-min incubation on noncoated, collagen I–, fibronectin-, and laminin-coated 12-well culture plates, the culture medium was aspirated, and the plates were washed twice with PBS. Adhesive cells were stained with Wright Giemsa solution. *B,* cell spreading on fibronectin was enhanced in PRL-1 knockdown cells compared with parental and control cells. Unspread cells were defined as phase-bright cells, whereas spread cells were flat and phase dark. Five fields were counted in three separate wells or dishes, and the experiments were repeated thrice (*A* and *B*). *Points,* mean; *bars,* SE. *C,* representative micrographs of SCR and 149i cells on fibronectin-coated dishes at 60 min.

examined DLD-1 colorectal cells after transient transfection and observed no difference in cell morphology and cell growth rate and a decrease in cell migration. Like Kato et al. (19), we found no significant difference in cell growth rate 48 h after cell plating. In contrast to Kato et al. (19), however, who only reported cell growth at one time point, we extended our study and found growth suppression 3 and 4 days after cell plating (Fig. 1*D*). We also examined cell migration at multiple time points and found that the initial migratory rate was elevated (Fig. 2*A*); we did not study cell migration at 48 h as did Kato et al. (19) but noted a saturation of cell migration at 24 h. It is possible that the difference between our results and those of Kato et al. (19) could reflect differences in the cell types or the methodologies employed. Nonetheless, both studies support an important role for PRL-1 in tumor cell adherence and invasion.

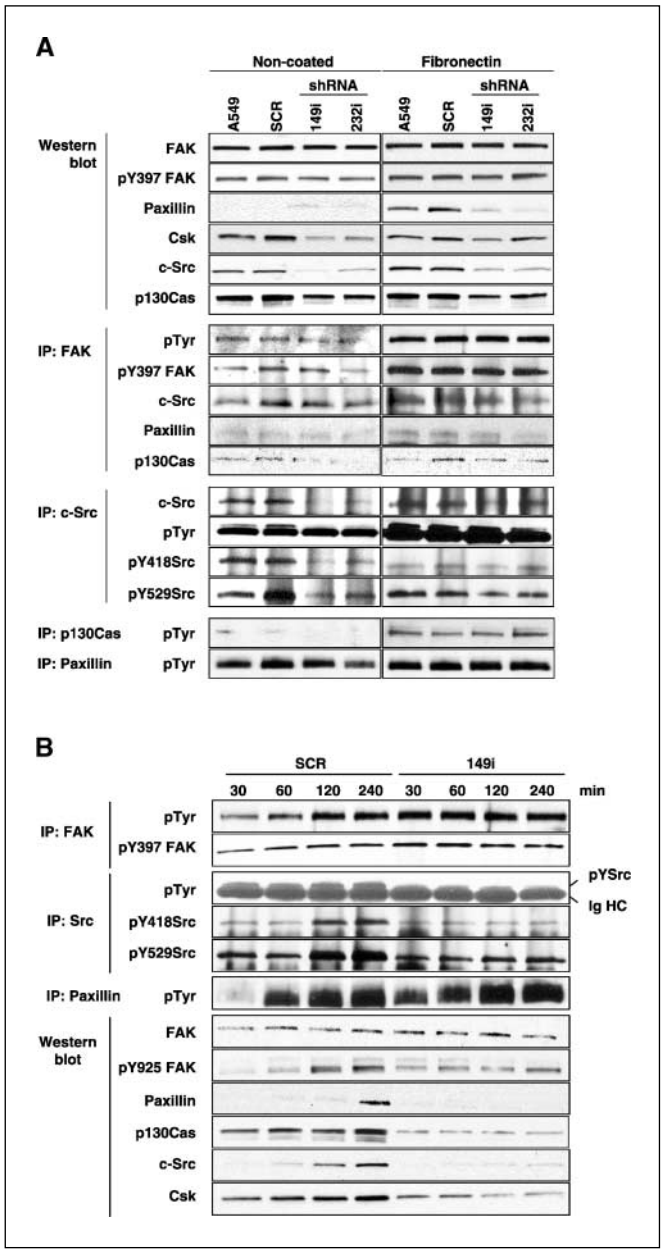

Fig. 4. Effect of PRL-1 knockdown of FAK, Src, paxillin, and p130Cas. *A,* cells were plated on noncoated or fibronectin-coated dishes and allowed to grow for 2 d to near confluence. Cells were then harvested for either Western blotting or immunoprecipitation. *B,* cells were plated on fibronectin-coated dishes and allowed to adhere for 30 to 240 min before being harvested for either Western blotting or immunoprecipitation to permit an analysis of the changes in FAK phosphorylation, Src, p130Cas, and paxillin levels.

To better explain the roles of PRL-1 in cell adhesion, spreading, and invasion, we focused on focal adhesion molecules and Rho family GTPases. Several phosphatases can control cell motility by modulating the phosphorylation status of focal adhesion molecules and cell-extracellular matrix interactions, which can alter actin cytoskeletal dynamics by regulating Rho family GTPase (3–5). For example, PTP-PEST dephosphorylates p130Cas and paxillin (21, 22). Tyrosine-phosphorylated paxillin recruits Crk to p130Cas (23–25), which enlists the Rac GEF DOCK180-ELMO complex (26, 27), leading to Rac-GTP and actin polymerization in lamellipodia. PTP-PEST have recently been reported to couple membrane protrusion and tail retraction in cell migration by acting on VAV2 and p190RhoGAP to reciprocally modulate the activity of Rac1 and RhoA (28). Several phosphatases are also involved in the regulation of Src family kinases (SFK), which play key roles in cell differentiation, proliferation, survival, and motility. The chief phosphorylation sites of SFKs are Tyr^{418}, which results in activation from autophosphorylation, and Tyr^{529}, which results in inhibition from Csk phosphorylation. Under physiologic condition, Csk is known to be an upstream negative regulator of SFKs (29, 30). Dephosphorylation of $pTyr^{529}$ increases SFKs activity. In our study, c-Src protein levels were decreased in PRL-1 knockdown cells. Initially, we thought PRL-1 knockdown might have influenced the c-Src tyrosine phosphorylation status, but our subsequent results indicated that fibronectin-stimulated regulation of c-Src phosphorylation status was independent of PRL-1 status. Furthermore, Csk expression correlated with c-Src expression (Fig. 4*A* and *B*), suggesting that PRL-1 was not directly associated with c-Src phosphorylation.

Upon extracellular matrix-integrin engagement, FAK autophosphorylation occurs at Tyr^{397}, which creates a binding motif that is recognized by various SH2-domain containing protein, including SFKs (31). In our study, FAK expression and tyrosine phosphorylation, including pY397 FAK, were similar in control and PRL-1 knockdown cells (Fig. 4*A*). Time course experiments showed that they increased in a time-dependent manner in SCR cells, whereas they were persistently elevated in PRL-1 knockdown cells (Fig. 4*B*). This was consistent with the notion that adhesion turnover was delayed or deficient in PRL-1 knockdown cells. Tyr^{925} of FAK has been reported to be a Src-dependent phosphorylation site, and Src is required for adhesion turnover associated with cell migration in cancer cells (32). Src-mediated phosphorylation of FAK at Tyr^{925} creates an SH2-binding site for the growth factor receptor–bound protein 2 (GRB2) adaptor proteins, which leads to the activation of Ras and the ERK2 cascade. The GRB2 and paxillin binding sites overlap and $pTyr^{925}$ FAK might be selectively released from focal adhesion complexes (33). In nearly confluent cells, there were no differences in total tyrosine phosphorylation or phosphorylation at Tyr^{397} of FAK between control and PRL-1 knockdown cells (Fig. 4*A*). On the other hand, in the early phase of cell adherence, both total tyrosine and Tyr^{397} FAK phosphorylation in SCR cells were increased in a time-dependent manner, but they showed persistently higher levels in 149i cells compared with SCR cells (Fig. 4*B*). Differences were also noted in the kinetics of Tyr^{925} phosphorylation on FAK. In SCR cells, time-dependent Tyr^{925} phosphorylation was seen after placement on fibronectin presumably

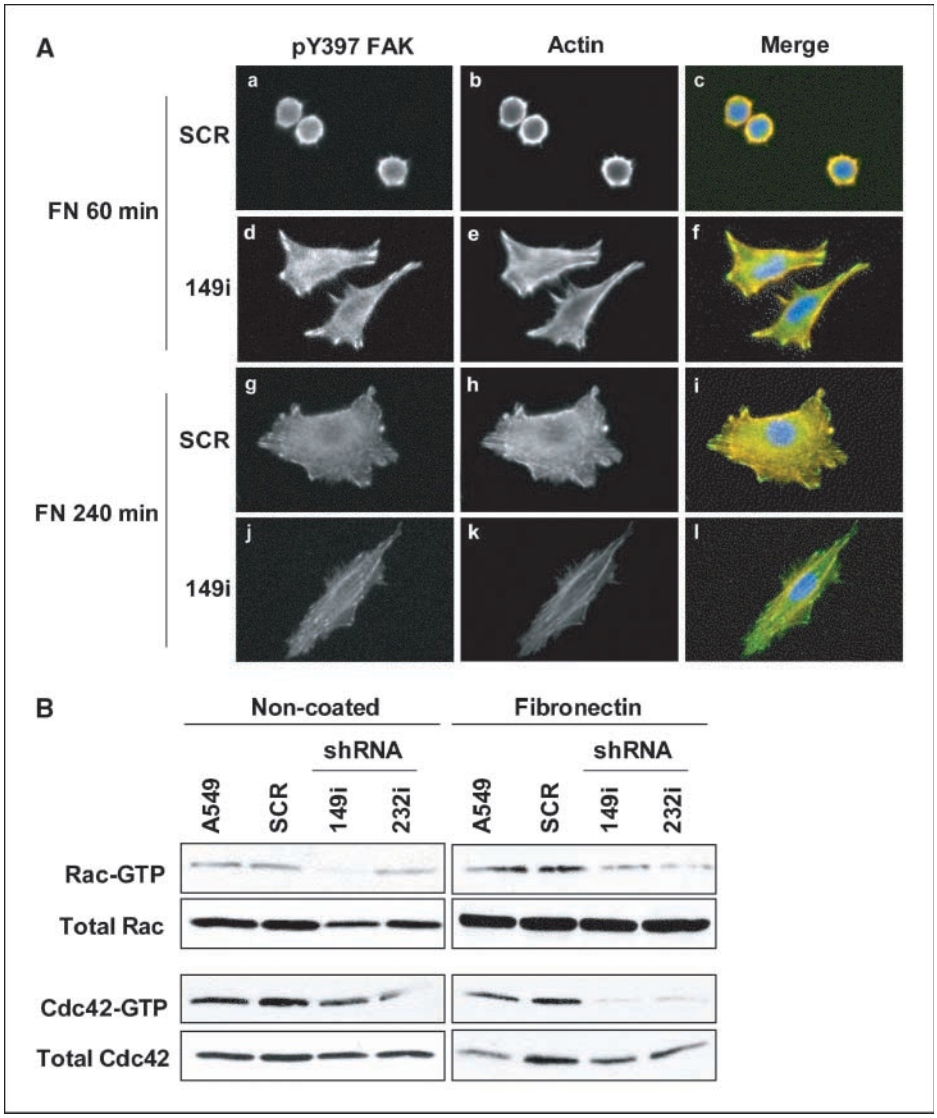

Fig. 5. PRL-1–depleted cells showed decrease lamellipodium extension and focal adhesion turnover with Rac and Cdc42 inactivation. *A,* SCR and 149i cells were plated on fibronectin-coated dishes and incubated for 60 min (*a–f*) and 240 min (*g–l*) and then stained for pTyr^{397} FAK (*green*) and filamentous actin (*red*). *B,* total or active Rac and Cdc42 were examined in lysates from cells grown for 2 d on fibronectin-coated or uncoated dishes.

due to Src activation (32), whereas PRL-1–depleted cells lacked significant phosphorylation of Tyr^{925} FAK in the early phase of cell adherence consistent with the lack of Src (Fig. 4*B*). This could contribute in FAK being localized persistently at focal adhesion complexes. Taken together, we speculate that the continuous FAK phosphorylation reflected decreased focal adhesion turnover.

Rac1 and Cdc42 activation were strongly inhibited in PRL-1–depleted cells placed on fibronectin. This suggests that PRL-1 was directly involved with Rac1 or Cdc42 activation. Rho family GTPases, such as Rac1 and Cdc42, play central roles in controlling cell migration and actin cytoskeletal reorganization. Rho GTPases are closely associated with regulation of integrin signals and adhesion turnover (34–37). Unexpectedly, reduction of PRL-1 increased cell spreading. Immunofluorescence of focal adhesion structure and actin organization suggested that focal adhesion staining was more diffusely spread in PRL-1 knockdown cells. The actin formation and lamellipodia extensions were decreased and seemed to lag behind focal adhesion after PRL-1 knockdown. The inhibition in Rac1 and Cdc42 activation after PRL-1 reduction would be consistent with delayed adhesion turnover and increased cell spreading due to continuous activation of focal adhesion complexes after PRL-1 knockdown.

Collectively, our results provide firm support for the involvement of PRL-1 in cell adhesion and migration processes via Rho family GTPases, which can regulate actin cytoskeletal rearrangement and focal adhesion turnover. Moreover, we document for the first time a functional role of PRL-1 in the processes of cell migration and invasion in non–small cell lung cancer. These findings suggest that therapies targeting PRL-1 may diminish the propensity for invasion and metastases in NSCLC.

Acknowledgments

Received 7/3/2006; revised 10/19/2006; accepted 11/16/2006.

Grant support: USPHS grant CA78039, pilot grant for the University of Pittsburgh Lung Specialized Programs of Research Excellence CA90440, Fiske Drug Discovery Fund, and Japanese Clinical Pharmacology Research Foundation fellowship (H. Achiwa).

The costs of publication of this article were defrayed in part by the payment of page charges. This article must therefore be hereby marked *advertisement* in accordance with 18 U.S.C. Section 1734 solely to indicate this fact.

We thank Robert Tomko and Dr. Brian Reese for thoughtful comments.

References

1. Jemal A, Murray T, Ward E, et al. Cancer statistics 2005. Ca Cancer J Clin 2005;55:10–30.
2. Stetler-Stevenson WG. Invasion and metastases. In: DeVita VT, Hellman S, Rosenberg SA, editors. Cancer: principles & practice of oncology, 7th edition.
3. Östman A, Hellberg C, Böhmer FD. Protein-tyrosine phosphatases and cancer. Nat Rev Cancer 2006;6:307–20.
4. Larsen M, Tremblay ML, Yamada KM. Phosphatases in cell-matrix adhesion and migration. Nat Rev Mol Cell Biol 2003;4:700–11.
5. Burridge K, Sastry SK, Sallee JL. Regulation of cell adhesion by protein-tyrosine phosphatases. 1. Cell-matrix adhesion. J Biol Chem 2006;281:15593–6.
6. Stephens BJ, Han H, Gokhale V, Von Hoff DD. PRL phosphatases as potential molecular targets in cancer. Mol Cancer Ther 2005;4:1653–61.
7. Mohn KL, Laz TM, Hsu JC, Melby AE, Bravo R, Taub R. The immediate-early growth response in regenerating liver and insulin-stimulated H-35 cells: comparison with serum-stimulated 3T3 cells and identification of 41 novel immediate-early genes. Mol Cell Biol 1991;11:381–90.
8. Zeng Q, Hong W, Tan YH. Mouse PRL-2 and PRL-3, two potentially prenylated protein tyrosine phosphatases homologous to PRL-1. Biochem Biophys Res Commun 1998;244:421–7.
9. Saha S, Bardelli A, Buckhaults P, et al. A phosphatase associated with metastasis of colorectal cancer. Science 2001;294:1343–6.
10. Bardelli A, Saha S, Sager JA, et al. PRL-3 expression in metastatic cancers. Clin Cancer Res 2003;9:5607–15.
11. Diamond RH, Peters C, Jung SP, et al. Expression of PRL-1 nuclear PTPase is associated with proliferation in liver but with differentiation in intestine. Am J Physiol 1996;271:G121–9.
12. Wang J, Kirby CE, Herbst R. The tyrosine phosphatases PRL-1 localized to the endoplasmic reticulum and the mitotic spindle and is required for normal mitosis. J Biol Chem 2002;277:46659–68.
13. Zeng Q, Si X, Horstmann H, Xu Y, Hong W, Pallen CJ. Prenylation-dependent association of protein-tyrosine phosphatases PRL-1, -2, and -3 with the plasma membrane and the early endosome. J Biol Chem 2000; 275:21444–52.
14. Werner SR, Lee PA, DeCamp MW, Crowell DN, Randall SK, Crowell PL. Enhanced cell cycle progression and down regulation of p21(Cip1/Waf1) by PRL tyrosine phosphatases. Cancer Lett 2003;202:201–11.
15. Zeng Q, Dong JM, Guo K, et al. PRL-3 and PRL-1 promote cell migration, invasion, and metastasis. Cancer Res 2003;63:2716–22.
16. Cates CA, Michael RL, Stayrook KR, et al. Prenylation of oncogenic human PTP(CAAX) protein tyrosine phosphatases. Cancer Lett 1996;110:49–55.
17. Diamond RH, Cressman DE, Laz TM, Abrams CS, Taub R. PRL-1, a unique nuclear protein tyrosine phosphatase, affects cell growth. Mol Cell Biol 1994;14: 3752–62.
18. Fiordalisi JJ, Keller PJ, Cox AD. PRL tyrosine phosphatases regulate Rho family GTPases to promote invasion and motility. Cancer Res 2006;66:3153–61.
19. Kato H, Semba S, Miskad UA, Seo Y, Kasuga M, Yokozaki H. High expression of PRL-3 promotes cancer cell motility and liver metastasis in human colorectal cancer: a predictive molecular marker of metachronous liver and lung metastases. Clin Cancer Res 2004;10: 7318–28.
20. Peng L, Jin G, Wang L, Guo J, Meng L, Shou C. Identification of integrin alpha1 as an interacting protein of protein tyrosine phosphatase PRL-3. Biochem Biophys Res Commun 2006;342:179–83.
21. Shen Y, Schneider G, Cloutier J, Veillette A, Schaller M. Direct association of protein-tyrosine phosphatase PTP-PEST with paxillin. J Biol Chem 1998;273: 6474–81.
22. Garton A, Flint A, Tonks N. Identification of p130Cas as a substrate for the cytosolic protein tyrosine phosphatase PTP-PEST. Mol Cell Biol 1996;16:6408–18.
23. Salgia R, Pisick E, Sattler M, et al. p130Cas forms a signaling complex with the adapter protein CRKL in hematopoietic cells transformed by BCR/ABL oncogene. J Biol Chem 1996;271:25198–203.
24. Klemke RL, Leng J, Molander R, Brooks PC, Vuori K, Cheresh DA. CAS/Crk coupling serves as a "Molecular Switch" for induction of cell migration. J Cell Biol 1998; 140:961–72.
25. Lamorte L, Rodrigues S, Sangwan V, Turner CE, Park M. Crk associates with a multimolecular Paxillin/GIT2/β-PIX complex and promotes Rac-dependent relocalization of Paxillin to Focal contacts. Mol Biol Cell 2003;14: 2818–31.
26. Brugnera EB, Haney L, Grimsley C, et al. Unconventional Rac-GEF activity is mediated through the Dock180-ELMO complex. Nat Cell Biol 2002;4:574–82.
27. Côté JF, Vuori K. Identification of an evolutionarily conserved superfamily of DOCK180-related proteins with guanine nucleotide exchange activity. J Cell Sci 2002;115:4901–13.
28. Sastry SK, Rajfur Z, Lin BP, Cote JF, Tremblay M, Burridge K. PTP-PEST couples membrane protrusion and tail retraction via VAV2 and p190RhoGAP. J Biol Chem 2006;281:11627–36.
29. Hata A, Sabe H, Kurosaki T, Takata M, Hanafusa H. Functional analysis of Csk in signal transduction through the B-cell antigen receptor. Mol Cell Biol 1994;14:7306–13.
30. Chong YP, Mulhern TD, Cheng HC. C-terminal Src kinase (CSK) and CSK-homologous kinase (CHK): endogenous negative regulators of Src-family protein kinases. Growth Factors 2005;23:233–44.
31. Calalb MB, Polte TR, Hanks SK. Tyrosine phosphorylation of focal adhesion kinase at sites in the catalytic domain regulates kinase activity: a role for Src family kinases. Mol Cell Biol 1995;15:954–63.
32. Brunton VG, Avizienyte E, Fincham VJ, et al. Identification of Src-specific phosphorylation site on focal adhesion kinase: dissection of the role of Src SH2 and catalytic function and their consequences for tumor cell behavior. Cancer Res 2005;65:1335–42.
33. Mitra SK, Hanson DA, Schlaepfer DD. Focal adhesion kinase: in command and control of cell motility. Nat Rev Cell Biol 2005;6:56–68.
34. Clark EA, King WG, Brugge JS, Symons M, Hynes RO. Integrin-mediated signals regulated by members of Rho family of GTPases. J Cell Biol 1998;142: 573–86.
35. Schmitz AA, Govek EE, Bottner B, van Aelst L. Rho GTPases: signaling, migration, and invasion. Exp Cell Res 2000;261:1–12.
36. Wennerberg K, Der CJ. Rho-family GTPases: it's not only Rac and Rho (and I like it). J Cell Sci 2004;117:1301–12.
37. Frank SR, Adelstein MR, Hansen SH. GIT2 represses Crk- and Rac1-regulated cell spreading and Cdc42-mediated focal adhesion turnover. EMBO J 2006;25: 1848–59.

PRL-1 Tyrosine Phosphatase Regulates c-Src Levels, Adherence, and Invasion in Human Lung Cancer Cells

Hiroyuki Achiwa and John S. Lazo

Cancer Res 2007;67:643-650.